Removing upwind/downwind ambiguity of ocean wind direction by polarimetric microwave radiometer: scheme design on on-orbit calibration and scanning geometry

WANG Zhen-zhan, LIU Jing-yi, YIN Xiao-bin, JIANG Jing-shan

Center for Space Science and Applied Research, Chinese Academy of Sciences, Beijing 100190, China

Abstract: Polarimetric microwave radiometer, a new type of remote sensor, can measure not only the first two Stokes parameters but also the third and the fourth Stokes parameter of ocean surface radiation. Thus it opens a new field of microwave remote sensing on wind vectors. There is wind direction ambiguity in actually retrieved oceanic wind field using fully polarimetric radiometer data because wind direction signals in T_v and T_h are very small comparing with other geophysical parameters, while T_3 and T_4 are basically two order smaller than those of horizontal and vertical polarization, and meanwhile there are calibration errors in each Stokes parameters. In this paper, we dedicate to improve the calibration accuracy by designing a fully onboard calibrator and reasonably allocating time for calibration and observation during one scan cycle. The theory of polarimetric microwave radiometer calibration is given and the actual considerations of the on-board fully polarimetric calibration standard are demonstrated. An original idea of calibrating polarimetric radiometer on satellite is presented. The relation between scan mode and wind direction retrieval error is analyzed. A new scanning geometry to remove these wind direction ambiguous solutions is devised and modeled. Simulation results show this kind of scanning geometry can remove wind direction ambiguity effectively. The accuracy of wind direction retrieval can be improved to 15°. On the other hand, due to the limited space on satellite, the swath of a single side scan can reach above 760 kilometers.

Key words: polarimetric microwave radiometer, ocean wind direction ambiguity, onboard calibration, scanning geometry

CLC number: TP732.1 Document code: A

1 INTRODUCTION

Since Skylab and Seasat Satellite launched in 1970's, microwave radiometer has become a main sensor to measure wind speed. As the sensitivity and calibration accuracy of microwave radiometer are improved, it has detected that sea surface brightness temperature is variable between 0.5K and 5K with different relative wind direction (Wentz, 1992). The followed research show that there were wind direction signals in both T_v and T_h, which can be used to retrieve the cosine of relative wind direction (Yuen, 1997; Meissner, 2002). However, a more accurate wind direction retrieval needs the aids of other data from scatter or global weather forecast data.

Polarimetric microwave radiometer, a new type of remote sensor, can measure not only the target's radiation, but also its polarizability. The correlation signals of the third and fourth stokes parameter in the ocean surface emissions vary periodly with relative wind direction. Thus they can be used to measure wind field more accurately. Polarimetric radiometer realizes utilization of all information about electromagnetic wave, including frequency, phase, amplitude and polarization. Therefore, in ocean remote sensing, it can measure many parameters, such as air, cloud, liquid water, sea surface temperature, wind vector, and so on.

In January 2003, the WindSat/Coriolis mission deployed the first spaceborne fully polarimetric passive microwave radiometer. The purpose of the mission is to demonstrate the capacity to obtain near-surface winds over the global oceans from passive microwave measurements (Gaiser, 2004). Its practicability has been tested by a lot of satellite data (Bettenhausen, 2006; Yueh, 2006). Due to some improper configurations of Windsat's scanning geometry, wind direction accuracy can not fully satisfy the measuring requirement of 20° (Laws, 2006; Wentz, 2005). A new

Received date: 2007-11-05; Accepted date: 2008-05-13

First author biography: WANG Zhen-zhan(1969—), received PH. D in Aug. 2005 in polarimetric microwave remote sensing of oceanic wind vector-principle, system design and application. His major interest is in microwave radiometer remote sensing of oceanic geophysical parameters, especially in its calibration and validation, retrieval algorithm development, surface emission and scattering models, and other related application studies in ocean and atmosphere parameter. He has taken part in many space-borne sensor's calibration, validation and application study programs, such as SZ-4 M^{3}RS, FY-3 MHS T/V calibration, and CE-1 MRM moon retrieval study, as well as HY-1, FY-1, FY-2 and SZ-3 optical sensor's in—situ calibration.

scan geometry of twice observation can remove wind direction ambiguity effectively, and improve the accuracy of wind direction retrieval up to 15° (Yin, 2008).

Calibration method and design scheme of polarimetric radiometer on satellite are presented. Time and space for calibration and observation during one scan cycle are reasonably allocated. A new scanning geometry to remove upwind/down wind direction errors due to ambiguous solutions is devised.

2 DESIGN ON ON-ORBIT CALIBRATOR OF FULLY POLARIMETRIC MICROWAVE RADIOMETER

Due to the cross-talk between polarimetric microwave radiometer's channels, channels unbalance exists. Two-point method can only calibrate every channel separately and can not reduce the unbalance error in the ortho-channel, which will weaken the calibration precision in the cross-polorization channels. Although often neglected in conventional radiometric measurements, the inter-channel cross-talk has to be accounted for in polarimetric radiometry due to its potential influence. Here we device a new method of end-to-end calibration for spaceborne polarimetric radiometer.

2.1 Principle on fully polarimetric microwave radiometer calibration

The relation between the antenna temperature of a fully polarimetric radiometer and its complete output can be written as (Lahtinen, 2003)

$$\bar{v}=\begin{bmatrix} v_1\\ v_2\\ v_3\\ v_4\end{bmatrix}=\begin{bmatrix} g_{vv} & g_{vh} & g_{v3} & g_{v4}\\ g_{hv} & g_{hh} & g_{h3} & g_{h4}\\ g_{3v} & g_{3h} & g_{33} & g_{34}\\ g_{4v} & g_{4h} & g_{43} & g_{44}\end{bmatrix}\begin{bmatrix} T_v\\ T_h\\ T_3\\ T_4\end{bmatrix}+\begin{bmatrix} o_v\\ o_h\\ o_3\\ o_4\end{bmatrix}+\bar{n}=\bar{\bar{g}}T_B+\bar{o}+\bar{n} \tag{1}$$

where $\bar{\upsilon}$ is video output response vector; $\bar{\bar{g}}$ and $\bar{o}$ consist of radiometer gain and offset parameters; and $\bar{n}$ is the instrument noise referred to the video outputs. The off-diagonal elements of $\bar{\bar{g}}$ represent inter-channel crosstalk, which can be the result of one or more hardware limitations. In order to invert the antenna brightness temperature vector from $\bar{\upsilon}$, the elements of $\bar{\bar{g}}$ and $\bar{o}$ in (1) are required. Estimates of these unknown gain and offset elements can be determined via fully polarimetric calibration, which requires the generation of at least five linearly independent brightness temperature vectors.

The fully polarimetric calibration standard can produce an infinite number of distinct linearly independent reference brightness vectors priorly with adequate precision and timeliness. This standard is composed of two parts (Fig. 1), one is a linearly polarized standard, which is formed by two blackbodies of different but precisely known emission temperatures along with a polarization-splitting wire grid, the other is a microwave phase retardation plate which is put between the linearly polarized standard and the radiometer antenna (Gasiewski, 1993; Lahtinen, 2003).

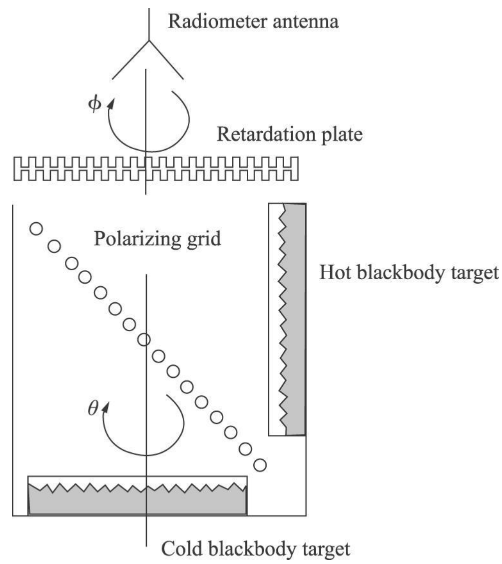

Fig. 1 Schematic diagram of a fully polarimetric calibration standard

The thorough analysis of the function principle of this calibrator proceeds by first calculating the tri-polarimetric Stokes vector of the linearly polarized standard, then multiplying this vector by a transformation matrix describing the influence of the retardation plate. The grid wire orientation angle measured with respect to the antenna polarization basis is θ. The rotation angle of the plate relative to the radiometer is ϕ. Changing θ, ϕ can produce many distinct calibration data matrix rows for precise calibration provided that the various material and component parameters of the standard are well known (vliet, 1981).

2.2 Design on on-orbit calibrator of fully polarimetric microwave radiometer

According to the theory of fully polarimetric calibration standard, we put forward a calibration method on satellite as shown in Fig. 2. Five angle combinations, including $\theta=0°$ and $\phi=0°$, $\theta=90°$ and $\phi=0°$, $\theta=45°$ and $\phi=0°$, $\theta=45°$ and $\phi=90°$, $\theta=30°$ and $\phi=90°$, produce five groups of fully polarimetric brightness temperatures. The cold calibration load is the mirror toward to the cold sky of 2.73K. The cold sky could enter into the calibration standard totally by adjusting the mirror's reflection angle. The hot calibration load is made of wide-band microwave absorber whose emissivity is close to 1. Its temperature can be measured by Pt resistance. The antenna reflector, feed and receiver are installed on a rotary platform to scan. The five fully polarimetric calibration standards are fixed between the reflector and feed. Five groups of grids and retarding plates are fixed to the five aforementioned angle combinations. As θ, ϕ, cold and hot temperatures are known, five groups of fully polarimetric brightness temperature are adequately known, which can be used to calibrate a space-borne fully polarimetric radiometer.

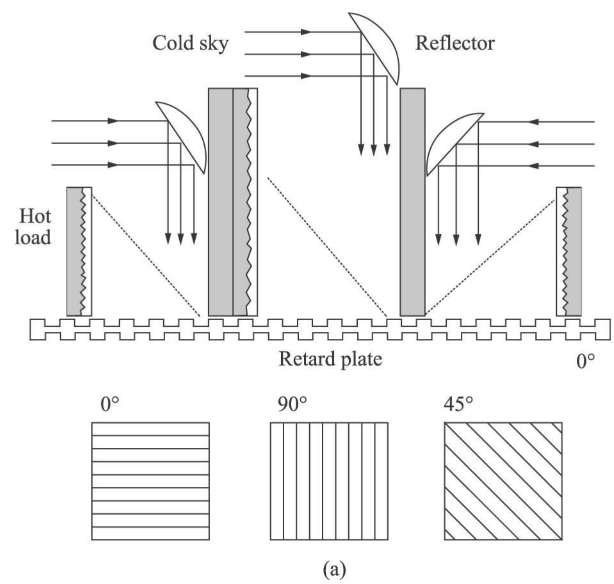

Fig. 2 Fully polarimetric calibration standard on-board

(a) Retard plate is 0°, wire grid is 0°, 90° and 45°; (b) Retard plate is 90°, wire grid is 45° and 30°

As the space is very limited on spaceship, the location of hot and cold calibration loads is very important. Since twice-scan needs low noise calibration standards should be set on the side of the satellite. But this will reduce the swath width of observing the earth. For once-scan, calibration standards can be set on any position among scan area or at the back of scan area. This can not affect the swath width. It is important for twice scan to designate where to observe the earth and where to calibrate during one scan cycle, and the swath must be wide enough at the same time. A new scan geometry will be given in section 4.

3 RELATIONSHIP BETWEEN WIND VECTOR RETRIEVALS AND SCANNING GEOMETRY OF SPACE-BORNE POLARIMETRIC MICRO-WAVE RADIOMETER

The wind vector retrieval results under various scanning geometries are discussed (Yin, 2008). They show that it is difficult to remove errors of wind direction ambiguous solutions in [0°, 30°], [150°, 200°] and [330°, 360°] with maximum-likelihood estimation (MLE) and once-scan data, as shown in Fig. 3(a). But most of wind direction ambiguous solutions can be removed with once-scan optimization method, as shown in Fig. 3(c), and the results are best with twice-scan optimization method, as shown in Fig. 3(e). The aforementioned conclusions are suitable for wind speed below 20m/s, as shown in Fig. 3(b), Fig. 3(d) and Fig. 3(f). The 3rd and 4th stokes parameters get stronger as wind gets harder. So the retrieval results are better in high wind speed.

As true wind direction couldn't be known in practical retrieval, once-scan optimization and twice-scan optimization methods couldn't be realized. However they confirm that when wind speed is up 7m/s and the 3rd and 4th stokes parameters' instrument and model errors are less than 0.4K and 0.25K separately, wind direction retrieval accuracy can be better than 20°.

The twice-scan can be realized based on conical-scan similar to that of AMSR (AMSR-E, 2004). And the difference of scan angle in two scans will change from 0° to 180° with different pixels of scan, as indicated by Fig. 4.

The relation between antenna scan azimuth angles ϕ_1 of forward-looking and ϕ_2 of backward-looking for the same ground cell is $\phi_1 + \phi_2 = 180°$. Suppose that ϕ_1 and ϕ_2 are measured clockwise from the same ground cell, the difference of scan angles (α) between for-look and aft-look for the same ground cell is $180 - 2 \times \phi_1$. The difference of scan angles (α) can also be calculated by

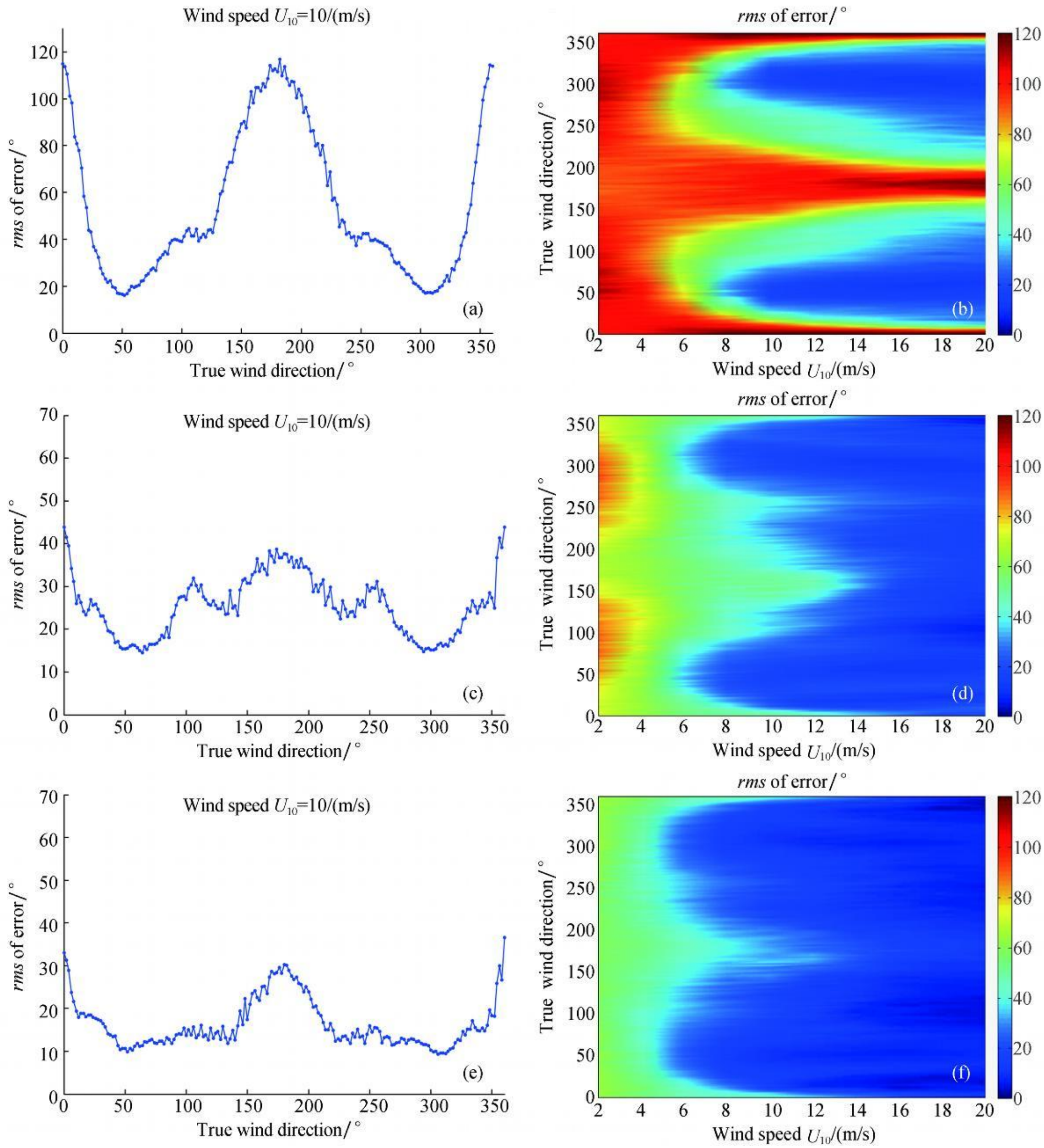

Fig. 3 Wind direction error based on various algorithm as a function of the true wind Wind direction error based on once-scan MLE (a), once-scan optimization (c) and twice-scan optimization (e) as a function of the true wind direction Wind direction error based on once-scan MLE (b), once-scan optimization (d) and twice-scan optimization (f) as a function of the true wind direction and speed

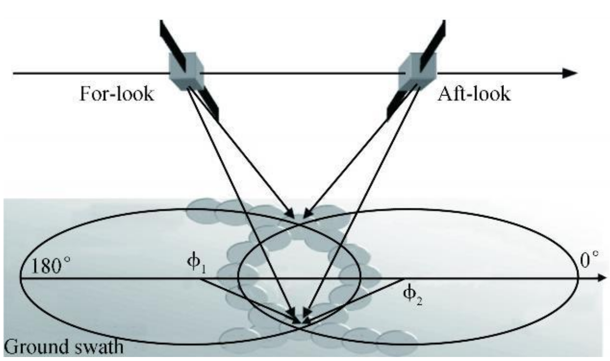

Fig. 4 Operation principle of twice-scan

$$\alpha = 2\arcsin\left(\frac{vT}{2r} \cdot n\right) \tag{2}$$

where v is velocity of sub-satellite point, T is period of one scan, r is radius of ground swath, and n is the number of scan.

It is clear that each pixel on the ground swath will be scan twice by the forward looking of one scan and the backward looking of several scans later if parameters of conical-scan geometry are set properly. Fig. 5 shows the difference of scan angles α versus the number of scan, given that the height of satellite is 800km, the radius of earth is 6370km, the incidence angle is 47°, the ground resolution is 20km, and the period of one scan is 2.66 seconds.

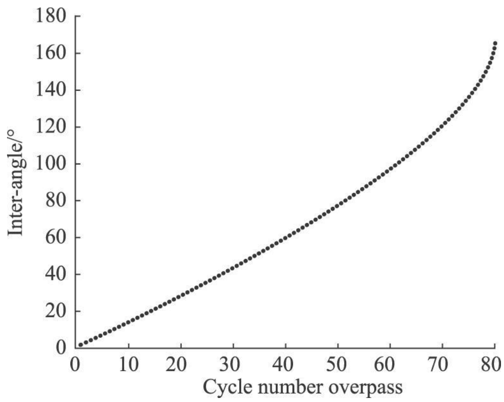

Fig. 5 The difference of scan angles α versus the number of scan

The same inter-angle of twice-scan pixels locate parallelly to the satellite orbit, as shown in Fig. 6.

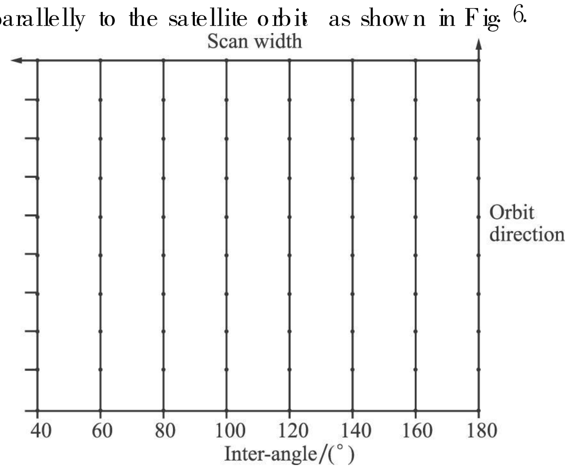

Fig. 6 Scan angles α as scan width

The algorithm based on closest solution of two scans shows different performances of removing upwind/downwind ambiguity as the angle α changes. When true wind direction is in the area of 0°—20° and 340°—360°, this algorithm is good for removing upwind/downwind ambiguity as the angle α changes from 20° to 80°; When true wind direction is in the area of 160°—200°, this algorithm performance is better for the angle α from 80° to 140°, as indicated by Fig. 7.

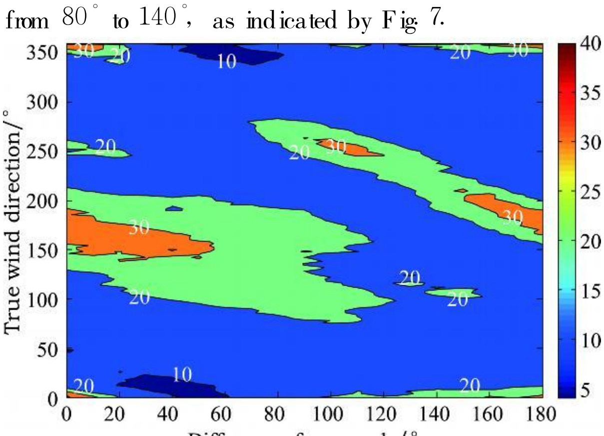

Fig. 7 Errors of retrieved wind direction versus α relative to the true wind direction

Fig. 8(a) shows the angle α of different fore-look cells in one scan, and Fig. 8(b) shows corresponding error for each cell with true wind direction being 0°. The cells near the position that along or perpendicular to spacecraft-heading vector give the largest error of retrieved wind direction, as indicated by Fig. 8(b). Thus these cells can be used for cold and warm calibration, and the other pixels which give smaller direction errors can be used for wind direction remote sensing, as indicated by Fig. 9.

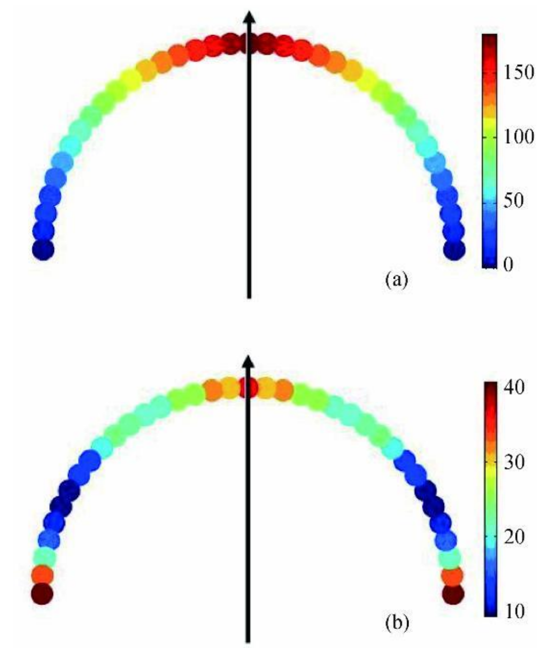

Fig. 8 Characters of for-look cells
(a) Angle α of different for-look cells;
(b) Error in different cell with true wind direction being 0°

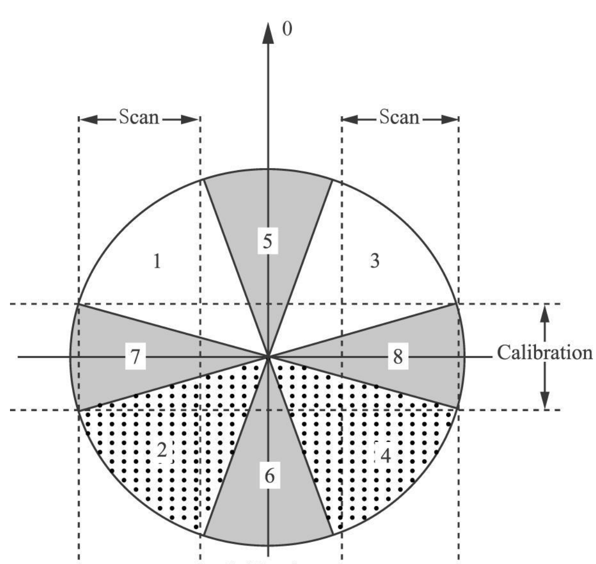

Fig. 9 New scanning geometry

4 DESIGN ON SCHEME OF ON-ORBIT CALIBRATION AND SCANNING GEOMETRY

The difference of scan angles α between for-look and aft-look varies from 0° to 180° for different scan cell. It is an important to choose where to observe the earth and where to calibrate during one scan. An example of arranging microwave radiometer's scan cell and calibration cell is shown in Fig. 9. Area 1, 2, 3 and 4 can be used to observe the earth. Its scan angle is from 10° to 80° in a quarter of one cycle. Area 5, 6, 7 and 8 can be used to set calibration standards. Its scan angle is from 0° to 10° and 80° to 90°. Area 1 and 2 or area 3 and 4 can be combined to fulfill for-look and aft-look observations. Area 5 and 6 or area 7 and 8 can be combined to set calibration standards.

Actually antenna and feed may be blocked by the satellite in per scan due to radiometer and antenna's position and calibration body size. Area 1, 2, 3 and 4 can't be used for observing the earth totally. Observation can be designed on one side of instrument to make antenna not be shielded during half of one cycle and get enough width for fore-scan and aft-scan swath to 750 km, which will cover the wind field globally in a short period. A detailed parameter setted for observation geometry will be estimated later according to requirements of wind vector remote sensing and level of instrumental noises as well as GMF model errors.

5 SUMMARIES AND CONCLUSIONS

According to the new algorithm of removing fully polarimetric radiometer's upwind/downwind direction errors due to ambiguous solutions, a new scan geometry with fore and aft twice look at the same cell is put forward. Scan geometry and calibration scheme of on-board polarimetric radiometer in one scan cycle are assigned.

Estimates of unknown gain and offset elements in a polarimeter system can be determined via fully polarimetric calibration, which requires the generation of at least five linearly independent brightness temperature vectors. The source designs and stability of cold load, the angle accuracy of grid and retarding plate are the key to calibration accuracy accurately on-board. Five groups of angle combinations will produce five groups of polarimetric brightness temperature. They will be used for calculating all the unknown gain and offset.

As the difference of scan angles α between for-look and aft-look is different for the same cell, the ability to remove ambiguous solutions is different. When the relative wind direction is ranging ranging from 0° to 20° and from 340° to 360°, and α from 20° to 80°, or the relative wind direction is ranging from 160° to 200°, and α from 80° to 140°, wind direction retrieval error is the least. When scan line is parallel or perpendicular to the satellite moving direction, wind direction retrieval error is the biggest. Allotting observation and calibration positions reasonably can improve not only calibrating precision but also retrieval accuracy.

REFERENCES

AMSR-E data users handbook. 2006. Japan Aerospace Exploration Agency, Japan

Bettenhausen M H, Smith C K, Bevilacqua R M, et al. 2006. A nonlinear optimization algorithm for windsat wind vector retrievals. IEEE Transactions on Geoscience and Remote Sensing, **44** (3): 597–608

Gaiser P W, St Germain K M, Twarog E M, et al. 2004. The WindSat spaceborne polarimetric microwave radiometer: sensor description and early orbit performance. IEEE Transactions on Geoscience and Remote Sensing, **42** (11): 2347–2361

Gasiewski A J and Kunkee D B. 1993. Calibration and application of polarization correlating radiometers. IEEE Transactions Microwave Theory and Techniques, **41** (5): 767–773

Lahtinen J, Gasiewski A J, Klein M, et al. 2003. A calibration method for fully polarimetric microwave radiometers. IEEE Transactions on Geoscience and Remote Sensing, **41** (3): 588–602

Lahtinen J and Hallikainen M. 2003. HUT fully polarimetric calibration standard for microwave radiometry. IEEE Transactions on Geoscience and Remote Sensing, **41** (3): 603–611

Laws K E, Lyzenga D R, Wiberg D M, et al. 2006. Characterization of errors in vector wind retrievals from satellite-based polarimetric microwave radiometer measurements. IEEE Transactions on Geoscience and Remote Sensing Letters, **3** (1): 45–48

Liu J Y, Wang Z Z, Yin X B, et al. 2008. Ocean wind retrieval from the brightness temperature data of the WindSat microwave polarimetric radiometer. High Technology Letters, vol. **18** (5): 519–524

Meissner T and Wentz F. 2002. An updated analysis of the wind direction signal in passive microwave brightness temperatures. IEEE Transactions on Geoscience and Remote Sensing, **40** (6): 1230–1240

Vliet A H and de Graauw T. 1981. Quarter wave plates for submillimeter wavelengths. International Journal of Infrared and Millimeter Waves, **2** (3): 465–477

Wentz F. 1992. Measurement of oceanic wind vector using satellite microwave radiometers. IEEE Transactions on Geoscience and Remote Sensing, **30** (5): 960–972

Wentz F J, Meissner T and Smith D K. 2005. Assessment of the initial release of WindSat wind retrievals. RSS Technical Report, America

Yin X B, Wang Z Z, Liu J Y, et al. 2009. Removing upwind/downwind ambiguity of ocean wind direction by polarimetric microwave radiometer: algorithmic basis. Journal of Remote Sensing, in press

Yueh S H, Wilson W J, Li F K, et al. 1997. Polarimetric brightness temperatures of sea surfaces measured with aircraft K- and Ka-band radiometers. IEEE Transactions on Geoscience and Remote Sensing, **35** (5): 1177–1187

Yueh S H, Wilson W J, Dinardo S J, et al. 2006. Polarimetric microwave wind radiometer model function and retrieval testing for Windsat. IEEE Transactions on Geoscience and Remote Sensing, **44** (3): 584–596

一种消除全极化微波辐射计顺/逆风向遥感模糊性的新方案
——星上定标和扫描机制设计的有关考虑

王振占，刘璟怡，殷晓斌，姜景山

中国科学院空间科学与应用研究中心，北京 100190

摘 要: 从观测方式的角度出发，讨论消除全极化微波辐射计遥感风向(顺风/逆风)模糊性的具体实施方案，提出合理进行星上定标和对地观测的设计思想。在研究全极化辐射计星上外定标方法的基础上，依据消除海面风向反演模糊性的算法，提出一种采用侧视扫描的机制，设计了在星上实现全极化微波辐射计对同一面元进行前、后两次扫描的具体方案，给出了一种在扫描周期内合理分配观测方位角和定标单元的方法。模拟结果表明，采用这种机制可以有效消除全极化辐射计风向反演存在的顺/逆风 180°模糊，使风向反演精度大大提高。同时，考虑到卫星上空间资源的限制，单侧扫描刈幅宽度还能够达到 760km 以上，能够满足在较短的时间内覆盖全球的时间分辨率的要求。

关键词: 全极化微波辐射计，海面风场反演模糊性，星上定标，扫描机制